Water Research 242 (2023) 120131

Contents lists available at ScienceDirect

Water Research

journal homepage: www.elsevier.com/locate/watres

Chlorination of amides: Kinetics and mechanisms of formation of *N*-chloramides and their reactions with phenolic compounds

Tianqi Zhang [a], Urs von Gunten [a,b,*]

[a] School of Architecture, Civil and Environmental Engineering (ENAC), Ecole Polytechnique Fédérale de Lausanne (EPFL), Lausanne 1015, Switzerland
[b] Eawag, Swiss Federal Institute of Aquatic Science and Technology, Dübendorf CH-8600, Switzerland

ARTICLE INFO

Keywords:
Chlorine
Amides
N-chloramides
Phenolic compounds
Second-order rate constants
Activation energies

ABSTRACT

Amides are common constituents in natural organic matter and synthetic chemicals. In this study, we investigated kinetics and mechanisms of the reactions of chlorine with seven amides, including acetamide, *N*-methylformamide, *N*-methylacetamide, benzamide, *N*-methylbenzamide, *N*-propylbenzamide, and *N*-(benzoylglycyl) glycine amide. Apparent second-order rate constants for the reactions of the amides with chlorine at pH 8 are in the range of 5.8×10^{-3} – 1.8 $M^{-1}s^{-1}$ and activation energies in the range of 62-88 kJ/mol. The second-order rate constants for the reactions of chlorine with different amides decrease with increasing electron donor character of the substituents on the amide-*N* and *N*-carbonyl-*C* in the amide structures. Hypochlorite ($^{-}$OCl) dominates the reactions of chlorine with amides yielding *N*-chloramides with species-specific second-order rate constants in the range of 7.3×10^{-3} – 2.3 $M^{-1}s^{-1}$. Kinetic model simulations suggest that *N*-chlorinated primary amides further react with HOCl with second-order rate constants in the order of 10 $M^{-1}s^{-1}$. The chlorination products of amides, *N*-chloramides are reactive towards phenolic compounds, forming chlorinated phenols via electrophilic aromatic substitution (phenol and resorcinol) and quinone via electron transfer (hydroquinone). Meanwhile, *N*-chloramides were recycled to the parent amides. At neutral pH, apparent second-order rate constants for the reactions between phenols and *N*-chloramides are in the order of 10^{-4}-0.1 $M^{-1}s^{-1}$, comparable to those with chloramine. The findings of this study improve the understanding of the fate of amides and chlorine during chlorination processes.

1. Introduction

Amide-type structures are ubiquitous in (i) natural systems, in some amino acids (e.g., asparagine, glutamine) and in peptide bonds, and (ii) synthetic organic materials (e.g., plastics) and chemicals (e.g., pharmaceuticals, surfactants, pesticides) (Ghose et al., 1999; Hargreaves, 2003; Pico et al., 2004). Amides were also found enriched in dissolved organic matter (Leenheer and Croue, 2003) and wastewater effluent organic matter (Barber et al., 2001). Because amides are relatively stable structures, amide-containing synthetic chemicals or metabolites can be detected in surface water and groundwater (Berens et al., 2021; Bexfield et al., 2021; Ferrer et al., 2000; Kolpin et al., 1996). In drinking water treatment, acetamide and a range of haloacetamides can be formed and have been identified as emerging disinfection byproducts (DBPs) (Plewa et al., 2008). In general, nitrogenous DBPs including haloacetamides have been shown to be far more genotoxic and cytotoxic than currently regulated DBPs, such as trihalomethanes (Muellner et al., 2007; Stalter et al., 2016). Therefore, it is crucial to understand the fate of amides in water treatment, especially during application of chemical oxidants such as the widely used chlorine.

To date, there is little information on the fate of amides during chlorination mainly due to relatively slow kinetics of the reaction between chlorine and amides. The apparent second-order rate constants for the reactions of chlorine with amides at pH 7 are more than two orders of magnitude lower compared to neutral amines, reduced sulfur compounds, and activated aromatic compounds (Deborde and von Gunten, 2008). In contrast, owing to the slow kinetics, the presence of amides could potentially control chlorine residual concentrations for long contact times.

Similar to amines, chlorination of amides occurs at the nitrogen (Morris, 1967). However, because of the electron-withdrawing effect of the carbonyl moiety, the mechanisms are different from amines. An attack by hypochlorite ($^{-}$OCl) instead of hypochlorous acid (HOCl) is proposed as the predominant mechanism. The formation of a hydrogen

* Corresponding author at: School of Architecture, Civil and Environmental Engineering (ENAC), Ecole Polytechnique Fédérale de Lausanne (EPFL), Lausanne 1015, Switzerland.
E-mail address: urs.vongunten@epfl.ch (U. von Gunten).

https://doi.org/10.1016/j.watres.2023.120131
Received 22 March 2023; Received in revised form 18 May 2023; Accepted 24 May 2023
Available online 25 May 2023

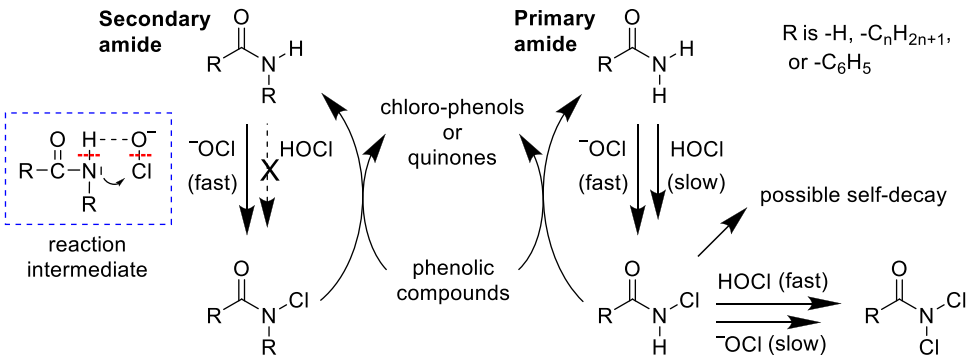

Scheme 1. Proposed mechanisms for the reactions of secondary (left) and primary (right) amides with chlorine and reactions of *N*-chloramides with phenolic compounds (middle). Dashed red lines represent the positions of bond cleavage. (For interpretation of the references to colour in this figure legend, the reader is referred to the web version of this article.)

bond between amido hydrogen and the oxygen in ⁻OCl was proposed as the initial step (Mauger and Soper, 1946; Thomm and Wayman, 1969), which enables the nitrogen to attack the partially positively charged chlorine, which leads to deprotonation and a release of hydroxide (Mauger and Soper, 1946) (Scheme 1, left). Compared with HOCl, the oxygen atom in ⁻OCl has a greater tendency to form a hydrogen bond because of its nucleophilic character. Another proposed mechanism suggests that the amido hydrogen dissociates slowly and the anionic structure of the amide resembling an enolate reacts with HOCl yielding a *N*-chloramide (Morris, 1978). *N*-chloramides formed during chlorination of amides have been observed to be capable to oxidize both inorganic and organic species, such as sulfite, thiosulfate, and organic sulfur and amine moieties (Ding et al., 2018; Prutz, 1999; Yu and Reckhow, 2017). Therefore, amides may serve as potential reservoirs of residual chlorine.

The aims of this study were to investigate kinetics and mechanisms of the reactions of chlorine with both primary and secondary amides and to elucidate the reactivity of chloramides with phenolic compounds. Kinetic experiments were conducted (i) in the pH range 7 to 10 to identify predominant reactive chlorine species (⁻OCl vs. HOCl) and (ii) in the temperature range 5 to 30 C to determine activation energies. During chlorination of primary amides, the evolutions of chlorine and chlorinated products were monitored experimentally and modeled using kinetic simulations to elucidate reaction mechanisms. The influence of bromide in the chlorination of amides was also theoretically assessed. Lastly, kinetics and mechanisms of *N*-chloramide reactions with the electron-rich moieties, phenol, catechol, resorcinol, and hydroquinone were investigated at pH 7 and 23 ℃.

2. Materials and methods

Chemicals and reagents. All chemicals and suppliers are provided in Table S1 (Supporting Information, SI). Table 1 lists the chemical structures of the seven selected amides, including acetamide (AA), *N*-

Table 1
Chemical structures of selected amides and their apparent (pH 8) and species-specific (⁻OCl) second-order rate constants for the reactions with chlorine.

Compound (abbreviation)	Structure	Apparent second-order rate constant at pH 8 (k_{app}, $M^{-1}s^{-1}$)	Species-specific second-order rate constant ($k_{\cdot OCl}$, $M^{-1}s^{-1}$)
Acetamide (AA)	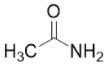	0.048	0.047
N-methylformamide (*N*-MFA)	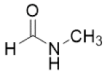	0.090	0.13, 0.21[a]
N-methylacetamide (*N*-MAA)	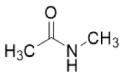	0.0087	0.013; 0.018[a]; 0.015[b]
Benzamide (BA)	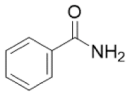	0.23	0.25
N-methylbenzamide (*N*-MBA)	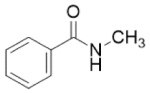	0.036	0.046; 0.042[c]
N-propylbenzamide (*N*-PBA)	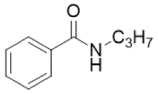	0.0058	0.0073
N-(benzoylglycyl)glycine amide (*N*-BGGA)	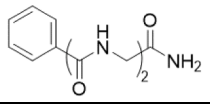	1.8	2.3

[a] Thomm and Wayman (1969);
[b] Antelo et al. (1995);
[c] Hardy and Robson (1967), measured at 20°C.

methylformamide (*N*-MFA), *N*-methylacetamide (*N*-MAA), benzamide (BA), *N*-methylbenzamide (*N*-MBA), *N*-propylbenzamide (*N*-PBA), and *N*-(benzoylglycyl)glycine amide (*N*-BGGA). AA and BA were recrystallized (for recrystallization protocols see Text S1, SI) before use due to observed interferences of impurities during kinetics measurements (Figures S1 and S2, SI). Ultra-purified water (Millipore system (18.2 MΩ)) was used to prepare all solutions. The concentration of sodium hypochlorite stock solutions was standardized weekly using a Shimadzu UV-1800 spectrophotometer ($\varepsilon_{\text{-OCl, 292 nm}} = 350\ M^{-1}cm^{-1}$) (Johnson and Melbourne, 1996; Wang et al., 1994).

Kinetic experiments for chlorination of amides. Kinetic experiments were conducted under pseudo-first-order conditions, i.e., measuring chlorine decrease in excess of amides, and/or measuring amides decrease in excess of chlorine (Corbett, 1972). In the experiments with excess amides, chlorine concentrations were measured via two different methods, (i) by direct photometry at 292 nm (for AA, *N*-MFA, and *N*-MAA), or (ii) by colorimetry with *N,N*-diethyl-*p*-phenylenediamine (DPD, for AA, BA, *N*-MBA, and *N*-PBA) (Baird and Bridgewater, 2017). In both cases, the experiments were conducted in cuvettes (Hellma Analytics) with temperature control of the cuvette holder (see below for details). For colorimetric measurements, samples were withdrawn and transferred to a second cuvette for quantification. In the experiments with excess chlorine, amide concentrations were measured using a Thermo Scientific HPLC-UV (Ultimate 3000) (for details see Text S2). In the experiments, no quenching reagent for chlorine was applied because the quenching reagents (e.g., thiosulfate, resorcinol) reduce *N*-chloramides back to the parent amides. Instead, reaction solutions were directly prepared in a HPLC vial, and samples were periodically injected into the HPLC system. The reaction time was calculated from the holding time in the autosampler to the injection of the compound (after injection, chlorine is separated quickly from the amide).

The kinetics of chlorine reactions with amides were assessed at different pH values (7, 8, 9, and 10) and different temperatures (5, 15, 23, and 30 °C). Phosphate (50 mM, pH 7 and 8) and borate (20 mM, pH 9 and 10) were applied to maintain the desired pH within ±0.05 units during the experiments. In experiments conducted in a cuvette, the temperature was controlled using a thermal bath (Büchi, F-108) connected to a cuvette holder in the spectrophotometer. In experiments conducted in HPLC vials, the temperature was controlled by the autosampler (Ultimate 3000). In experiments to measure chlorine decrease photometrically at low temperatures (5 and 15 °C), dry air was supplied continuously surrounding the cuvette to avoid water vapor condensation on the cuvette.

Identification of the formation of N-Cl-BA. During chlorination of BA, the formation of *N*-Cl-BA was confirmed using an Orbitrap LC-MS (Orbitrap Exploris 120, Thermo Fisher) by detecting the accurate mass of the *N*-Cl-BA cation ($C_7H_6ONCl+H^+$) and the isotope pattern of the chlorine atom ($C_7H_7ON^{35}Cl^+$ and $C_7H_7ON^{37}Cl^+$) at pH 7 and 10 (Text S3, Fig. S4). Dichloro-BA was not detected.

Preparation and quantification of N-chloramides. *N*-Chloramides were prepared by mixing chlorine with a 10-fold molar excess of amides and used after >99.9% of chlorine was consumed. *N*-Chloroacetamide (*N*-Cl-AA), a primary chloramide, was prepared in 20 mM borate buffer at pH 10 to avoid further consumption of *N*-Cl-AA by hypochlorous acid (HOCl). *N*-Chlorinated secondary amides were prepared in 50 mM phosphate buffer at pH 8. *N*-Chloramides were measured colorimetrically using DPD in presence of iodide which was adapted from halamine measurements (Baird and Bridgewater, 2017). Iodide doses in the range of 0.02-0.2 mM were applied depending on the rate of color formation (maximum absorbance was recorded at ~3 min).

N-Cl-*N*-MBA was used as a standard to validate the colorimetric method and to quantify other *N*-chloramides. First, *N*-Cl-*N*-MBA was converted to *N*-MBA with excess sodium thiosulfate and quantified using HPLC-UV by comparing it with the authentic standard of *N*-MBA. Then, the standardized *N*-Cl-*N*-MBA was used to generate a calibration curve with DPD and iodide which agreed well with a calibration curve of monochloramine using the same colorimetric method (Fig. S5). To quantify other *N*-chloramides, including *N*-Cl-AA, *N*-Cl-*N*-MFA, *N*-Cl-*N*-MAA, and *N*-Cl-BA, the photometric calibration curve of *N*-Cl-*N*-MBA was used by assuming the same absorbance response from different *N*-chloramides with the same concentration.

To investigate the reaction mechanisms of the chlorination of primary amides (AA, BA) both free chlorine and chlorinated amides were measured by the DPD method. First, chlorine was measured directly by adding DPD. Thereafter, *N*-Cl-AA (or *N*-Cl-BA) was measured in the same sample by addition of iodide and subtracting the absorbance induced by chlorine.

Kinetics and mechanisms for the reactions of N-chloramides with phenolic compounds. Phenol, catechol, resorcinol, and hydroquinone were investigated for their reactivity with the three different *N*-chloramides, *N*-Cl-AA, *N*-Cl-*N*-MAA, and *N*-Cl-*N*-MBA. The *N*-chloramides were prepared and standardized on a daily basis. Kinetics experiments for the reactions between *N*-Cl-AA (or *N*-Cl-*N*-MAA) and phenolic compounds were conducted with *N*-chloramides in excess by monitoring the abatement of the phenolic compounds by HPLC-UV (for more details see Text S2). The kinetics for the reactions between *N*-Cl-*N*-MBA and phenolic compounds were measured with phenols in excess by monitoring the decrease of *N*-Cl-*N*-MBA by HPLC-UV (Text S2). The kinetic experiments for the reactions of *N*-chloramides with phenols were conducted in a HPLC vial without applying a quenching agent. All experiments were conducted in duplicates.

To understand mechanisms, products of the reaction of *N*-chloroacetamide with phenolic compounds were detected using HPLC-UV (Text S2). In this part of the study, *N*-Cl-AA was prepared with a chlorine to acetamide molar ratio of 1:1.25 instead of 1:10 to minimize the interference of excess acetamide on the detection of the phenolic reaction products.

Kinetic model. To elucidate the reactions occurring during chlorination of primary amides, reaction kinetics were simulated by considering the reactions listed in Table S2. The kinetic simulations were conducted by solving kinetic equations (Text S4) using the stiff differential equations solver ODE15s in MATLAB (based on Gear's method). To ensure the quality of calculation, absolute error tolerance of each solution component (i.e., species concentration) was set at least 4 orders of magnitude below its respective value (e.g., tolerance for [$^-$OCl] was set to 10^{-10} M when [$^-$OCl] $\geq 10^{-6}$ M).

3. Results and discussion

3.1. Kinetics of the reactions of chlorine with amides

Apparent (k_{app}) second-order rate constants for the reactions of chlorine with 7 selected amides at pH 8 were determined in the range of $5.8 \times 10^{-3}\ M^{-1}s^{-1}$ to $1.8\ M^{-1}s^{-1}$ under pseudo-first-order condition by measuring chlorine decrease in excess of the amides (Tables 1 and S3). Species-specific second-order rate constants ($k_{\text{-OCl}}$) for the reactions of the amides with $^-$OCl were obtained at pH 10 (pK_{HOCl} is 7.54 at 25 °C (Morris 1966)) to be in the range of $7.3 \times 10^{-3}\ M^{-1}s^{-1}$ to $2.3\ M^{-1}s^{-1}$ (Table 1). $k_{\text{-OCl}}$ for *N*-MFA, *N*-MAA, and *N*-MBA, are similar to $k_{\text{-OCl}}$ values obtained in previous studies (Table 1). $k_{\text{-OCl}}$ values for the selected amides show that electron-donating groups (e.g., alkyl group) at the amide-*N* and/or the *N*-carbonyl-*C* lower the second-order rate constants for the reactions with $^-$OCl, with $k_{-\text{OCl,AA}} > k_{-\text{OCl,}N\text{-MAA}}$, $k_{-\text{OCl,}N\text{-MFA}} > k_{-\text{OCl,}N\text{-MAA}}$, and $k_{-\text{OCl,BA}} > k_{-\text{OCl,}N\text{-MBA}} > k_{-\text{OCl,}N\text{-PBA}}$ (Figure S6). As discussed above, $^-$OCl reacts with amides as a nucleophile by forming a hydrogen bond between the oxygen in $^-$OCl and amido hydrogen. Electron-donating groups at the amide-*N* and/or the *N*-carbonyl-*C* partially compensate for the electron-withdrawing effect of the carbonyl group on the amide-*N*, yielding a stronger *N*-*H* bond with a lower tendency to form a hydrogen bond with $^-$OCl. *N*-BGGA ($k_{-\text{OCl,}N\text{-BGGA}} = 2.3\ M^{-1}s^{-1}$) with 3 amide groups was observed to have an almost 10-fold higher species-specific second-order rate constant for the

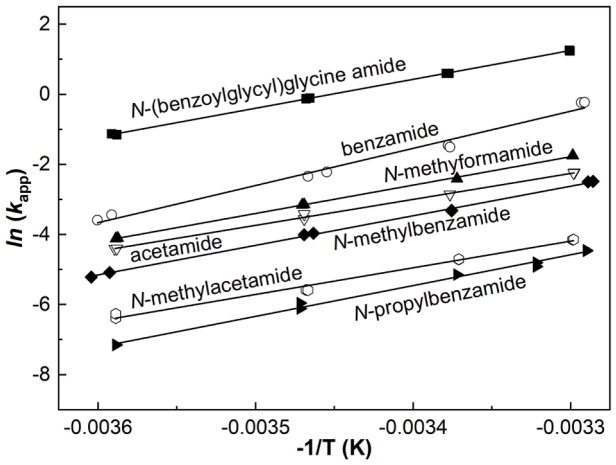

Fig. 1. Arrhenius plot for the determination of activation energies for the reactions of amides with chlorine. Logarithmic apparent second-order rate constants for the reactions of amides with chlorine as functions of the inverse temperatures at pH 8 (see equation 6 in the text). Lines are linear regressions. Table S4 provides detailed experimental conditions and the experimental values for this plot.

reaction with $^{-}$OCl than BA ($k_{-OCl,BA}$ = 0.25 $M^{-1}s^{-1}$) which can be explained by an increased electron withdrawing effect of the amide groups on neighboring amide-structures.

3.2. Activation energies for the reactions of amides with chlorine

To facilitate the implementation of second-order rate constants for realistic treatment conditions with varying temperatures (few°C to 30 °C), temperature-dependent kinetics of the reactions of amides with chlorine were investigated under pseudo-first-order conditions at 5, 15, 23, and 30 °C and at pH 8 (Table S4). Activation energies for these reactions were calculated using the logarithmized form of Arrhenius Eq. (6) (Arrhenius 1889; Logan 1982):

$$\ln k_{app} = \ln A - \frac{E_a}{R\,T} \quad (6)$$

where A is the pre-exponential factor, E_a is the activation energy, R is the universal gas constant (8.314 J mol^{-1} K^{-1}), and T is the absolute temperature (in K). E_a was obtained by plotting ln (k_{app}) as a function of -1/T (Fig. 1). A comparison of activation energies for the chlorination of various organic compounds is provided in Table 2. For the chlorination of the tested amides, E_a is in the range of 62-88 kJ/mol. Comparable E_a (61–69 kJ/mol) were reported for the chlorination of α,β-unsaturated carbonyls, e.g., tiglic aldehyde, trans-2-hexenal (Marron et al., 2021). In comparison, the chlorination of neutral amines and reduced sulfur moieties is less sensitive to temperature variation with E_a values from 14 kJ/mol for ametryn to 33 kJ/mol for cylindrospermopsin (Rodriguez et al., 2007; Xu et al., 2009). The E_a values for the chlorination of phenolic compounds and (polycyclic) aromatic compounds vary in a wide range from <2.5 kJ/mol for resorcinol to 58 kJ/mol for phenol and 59-62 kJ/mol for biphenyl (Lee and Morris, 1962; Rebenne et al., 1996; Snider and Alley, 1979). Amides (refer to the sections below) and α,β-unsaturated carbonyls (Marron et al., 2021) mainly react with $^{-}$OCl with relatively low second-order rate constants. In contrast, neutral amines/reduced sulfur and activated aromatic compounds (Deborde and von Gunten, 2008) mainly react with HOCl with higher second-order rate constants which potentially explain the observed E_a variations among different moieties. A weak correlation (R^2=0.54) was observed when plotting E_a vs. ln (k_{app}) which warrants further investigations (Fig. S7).

Table 2
Activation energies and apparent second-order rate constants for the chlorination of the investigated amides and other selected organic compounds.

Compound[a]	Activation energy (kJ/mol)	k_{app} at 20-25°C ($M^{-1}s^{-1}$)	pH	Reference
Amides				
Acetamide	62	4.8×10^{-2}	8	This study
N-methylformamide	67	9.0×10^{-2}	8	This study
N-methylacetamide	63	8.7×10^{-3}	8	This study
Benzamide	88	0.23	8	This study
N-methylbenzamide	70	3.6×10^{-2}	8	This study
N-propylbenzamide	73	5.8×10^{-3}	8	This study
N-(benzoylglycyl)glycine amide	68	1.8	8	This study
Phenacetin	58	0.45	7	Acero et al. (2010)
Olefins				
Microcystin-LR	20	72	7.2	Acero et al. (2005b)
Tiglic aldehyde	61	0.18	8	Marron et al. (2021)
Trans-2-hexenal	69	1.4	8	Marron et al. (2021)
Neutral amines and reduced sulfur moieties				
Ametryn	14	7.2×10^{2}	7	Xu et al. (2009)
Cylindrospermopsin	33	7.4×10^{2}	6.4	Rodriguez et al. (2007)
Nortriptyline	23	0.40	7	Acero et al. (2013)
Prometryn	32	8.3×10^{3}	7	Hu et al. (2021)
Aromatic compounds				
2-Benzyl-4-chlorophenol	32	28	7	Acero et al. (2013)
Bensulfuron-methyl	14	1.1×10^{3}	7	Hu et al. (2015)
Benzo(ghi)perylene	13	26	6.8	Harrison et al. (1976)
Biphenyl	59-62		N/A	Snider and Alley (1979)
Chlorimuron-ethyl	22	9.4	7	Hu et al. (2018)
Diazinon	30-36	0.48	10, 11	Zhang and Pehkonen (1999)
Naproxen	14	3.4	7	Acero et al. (2010)
Phenol	58		N/A	Lee and Morris (1962)
Pyrene	32	35	6.8	Harrison et al. (1976)
Resorcinol	$\leq$ 2.5	1.8×10^{2}	5	Rebenne et al. (1996)
Others				
Humic acid[b]	37		7	Urano et al. (1983)

[a] Compounds are grouped by reactive moieties with chlorine.
[b] Activation energy for the reaction of trihalomethanes formation from humic acid. N/A: not available.

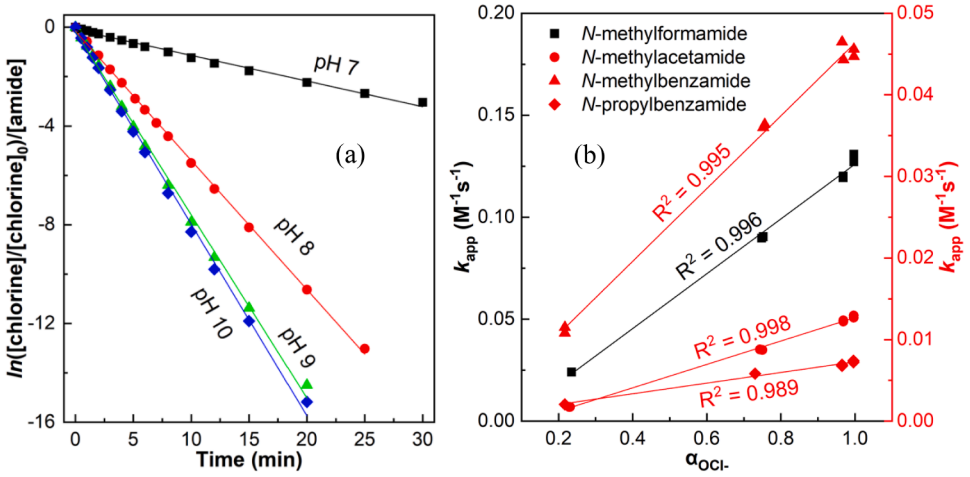

Fig. 2. pH-dependence of reactions of secondary amides with chlorine. (a) Logarithm of relative chlorine residual concentration normalized to the initial amide concentration in excess of *N*-methylacetamide as a function of time at different pH values and 23 °C. (b) Apparent second-order rate constants for reactions of secondary amides with chlorine as a function of α_{OCl^-} at 23 °C. Lines represent linear regressions and slopes in (a) are second-order rate constants. $[Chlorine]_0$ = 0.06-1.5 mM, $[amide]_0$ = 8–200 mM (more details are provided in Table S3).

3.3. Chlorination of secondary amides

Second-order rate constants for the reactions of chlorine with 4 secondary amides (*N*-MFA, *N*-MAA, *N*-MBA, *N*-PBA) were determined at different pH values (Figure S8). The reactions of secondary amides with chlorine exhibited pseudo-first-order kinetics with either chlorine or amides in excess and measuring the other reaction partner (Table S3). There are some differences (4-38%) in the apparent second-order rate constants (k_{app}) for the two experimental conditions (Figures S9). Such differences are small given the variation of reported second-order rate constants in literature of up to a factor of 10. For all tested secondary amides, k_{app} increased from pH 7 to 9, with no significant further increase to pH 10 (Figs. 2a and S8). When plotting k_{app} as a function of the fraction of hypochlorite (α_{OCl^-}) (only considering hypochlorous acid (HOCl) and $^-$OCl here) for different pH values, good linearities were observed for all tested secondary amides (Fig. 2b). This indicates an $^-$OCl-dominated chlorination of secondary amides. These findings support the proposed mechanism discussed in the introduction and shown in Scheme 1 (left). The same trend of $^-$OCl as a predominant chlorination species was also observed for *N*-BGGA, which contains 3 amide-*N* (Figure S10).

3.4. Chlorination of primary amides

Benzamide (BA). The kinetics of chlorination of BA were investigated at different pH values by measuring chlorine consumption in excess of BA and BA consumption in excess of chlorine. Pseudo-first-order kinetics were observed for both experimental conditions with good linearity for BA decrease (R^2 >0.99) and chlorine decrease (0.99> R^2 >0.97) (Table S3). Consistently higher k_{app} (23-45%) were observed when measuring chlorine decrease at different pH values (Figure S11a). When plotting k_{app} as a function of α_{OCl^-}, a better linearity was observed when measuring BA decrease (Figure S11b). Nevertheless, for the tested conditions, $^-$OCl seems the predominant species for the reaction of BA with chlorine. However, the lower linearity between k_{app} and α_{OCl^-} when measuring chlorine decrease in excess of benzamide indicates that besides $^-$OCl other chlorine species might contribute to BA abatement. In addition, different concentrations (1-9 mM) of chlorine were spiked to a 10 mM BA solution in the pH range 7-10. After complete chlorine consumption, roughly half of the molar equivalent of BA was consumed (Figure S12). The molar ratio of 2 to 1 for the reaction between chlorine and BA suggests that the BA chlorination product (*N*-Cl-BA) could further react with chlorine.

The role of chlorine monoxide (Cl_2O) and molecular chlorine (Cl_2) for chlorination of BA was also investigated owing to their high second-order rate constants for the reactions with different organic functional groups (Deborde and von Gunten, 2008; Li et al., 2020; Sivey et al., 2010). Cl_2O and Cl_2 are usually present at very low concentrations compared to HOCl and $^-$OCl. Based on the measured chloride concentration in the reaction solutions and known equilibria for the different chlorine species, their concentrations were calculated as a function of pH (Text S5). The highest concentrations of Cl_2O and Cl_2 were calculated at pH 7 and gradually decreasing up to pH 10 (Fig. S13). To assess the role of Cl_2O, the reaction order in chlorine was determined under pseudo-first-order conditions with varying chlorine concentrations (Text S6). When Cl_2O is a predominant chlorine species, the reaction rate is proportional to $[chlorine]^2$, and therefore, second-order kinetics relative to the chlorine concentration should be observed (Li et al., 2020; Sivey et al., 2010). As shown in Figure S14, first-order with respect to chlorine concentration was observed in the chlorination of BA at pH 7 (slope ~1) which indicates a minor role of Cl_2O. The role of Cl_2 for the chlorination of BA was assessed by spiking additional 10-100 mM Cl^- to 3 mM chlorine (containing already 6.3 mM Cl^- as background) which generated 8.7×10^{-9} - 5.7×10^{-8} M Cl_2 (Text S7). Accordingly, the observed pseudo-first-order rate constants (k_{obs}) for benzamide increased from 1.3×10^{-4} to 1.5×10^{-4} s^{-1} (Fig. S15a). Plotting k_{obs} as a function of Cl_2 concentration, $k_{Cl2,BA}$ was calculated to be 433 M^{-1}s^{-1} (Fig. S15b). However, considering the low concentrations of Cl_2 (<3.4×10^{-9} M) under the tested conditions, Cl_2 plays a negligible role in the chlorination of BA. Under typical drinking water chlorination conditions (e.g., [chlorine] = 2 mg/L as Cl_2, $[Cl^-]$ = 8 mg/L) (Li et al., 2020), Cl_2 has a concentration of less than 10^{-12} M at neutral pH and its role in the chlorination of amides can be neglected.

To further elucidate the mechanism of BA chlorination (Scheme 1, right), the formation of *N*-Cl-BA was first confirmed using high-resolution mass spectrometry (Figure S4) and then, the evolution of *N*-Cl-BA during chlorination of BA at different pH values was monitored with DPD and iodide (Fig. 3). *N*-Cl-BA was formed, and went through a maximum, followed by a decrease, due to a further reaction with chlorine (Mauger and Soper, 1946). In addition, it was observed that *N*-Cl-BA is unstable under the selected experimental conditions (Fig. S16). To better understand the reactions occurring during chlorination of BA (Scheme 1, right), a kinetic simulation of chlorine and *N*-Cl-BA evolution was performed by considering reactions (1) to (5) (Fig. 3):

$$RCONH_2 + {}^-OCl \rightarrow RCONHCl + {}^-OH \quad k_{\text{-OCl,BA}} = 0.25\ M^{-1}s^{-1} \quad (1)$$

$$RCONH_2 + HOCl \rightarrow RCONHCl + H_2O \quad k_{HOCl,BA} = 0.04\ M^{-1}s^{-1} \quad (2)$$

$$RCONHCl + {}^-OCl \rightarrow RCONCl_2 + {}^-OH \quad k_{\text{-OCl,}N\text{-Cl-BA}} = 1\ M^{-1}s^{-1} \quad (3)$$

$$RCONHCl + HOCl \rightarrow RCONCl_2 + H_2O \quad k_{HOCl,N\text{-Cl-BA}} = 10\ M^{-1}s^{-1} \quad (4)$$

$$RCONHCl \rightarrow \text{product} \quad k_{N\text{-Cl-BA}} = 2.4 - 4.2\ s^{-1} \text{ at pH 7-10} \quad (5)$$

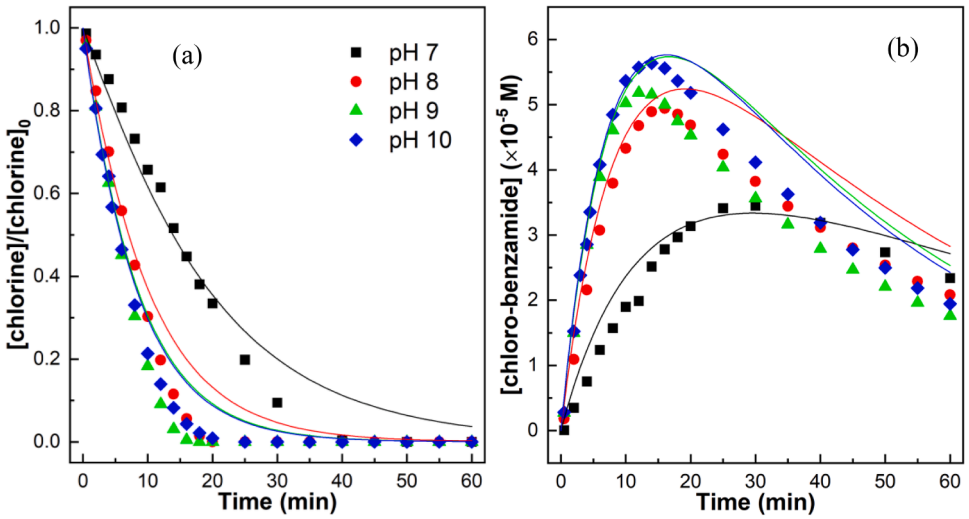

Fig. 3. Reaction of benzamide with chlorine at different pH values at 23 °C: Experimental data and modeling results. (a) Normalized chlorine residual concentration and (b) *N*-Cl-benzamide evolution. Lines represent model predictions (see text) and symbols are measured data. $[Chlorine]_0$ = 90 μM, $[benzamide]_0$ = 8 mM.

Among the rate constants, $k_{\text{-OCl,BA}}$ was obtained from the measured chlorine decrease in excess BA at pH 10 (Table S3). $k_{N\text{-Cl-BA}}$ was determined experimentally by measuring the *N*-Cl-BA decrease at different pH values after chlorine was completely consumed (Fig. S16, averaged values of slopes were taken from duplicate experiments at each pH). $k_{\text{-OCl},N\text{-Cl-BA}}$ was obtained by fitting to the formation of *N*-Cl-BA at pH 10 using $k_{\text{-OCl},N\text{-Cl-BA}}$ as a fitting parameter (Fig. S17). When fitting for $k_{\text{-OCl},N\text{-Cl-BA}}$ at pH 10, $k_{\text{HOCl,BA}}$ and $k_{\text{HOCl},N\text{-Cl-BA}}$ are irrelevant for the chlorine and *N*-Cl-BA evolution. Lastly, with the determined values for $k_{\text{-OCl,BA}}$, $k_{\text{-OCl},N\text{-Cl-BA}}$, and $k_{N\text{-Cl-BA}}$, $k_{\text{HOCl,BA}}$ and $k_{\text{HOCl},N\text{-Cl-BA}}$ were obtained by fitting the decrease of chlorine and the formation of *N*-Cl-BA at pH 7 simultaneously (Fig. S18). As shown in Figs. S17 and S18, different scenarios were tested to find the optimal values for the rate constants and the fit was selected by visual inspection. Applying the rate constants for reactions (1)-(5) (Table S2) for different pH conditions, the experimental and modeled chlorine and *N*-Cl-BA evolution were in good agreement up to a chlorine consumption of 70% (Fig. 3). The deviation in the later part of curves could be caused by additional reactions which were not considered in this study. To be noted, $^{-}$OCl dominates the reaction with BA, however, chlorine addition to BA makes the amide-*N* more acidic and therefore, a partial deprotonation may occur leading to a negative charge. This enables an electrophilic attack by HOCl (reaction 4). In analogy, a significant depression of the p*K*a values of several orders of magnitude has been calculated for chloramines relative to their amine precursors (Heeb et al., 2017).

Acetamide. The reaction mechanisms of the chlorination of AA were investigated analogously by measuring the chlorine decrease and *N*-Cl-AA evolution at different pH values (Fig. 4). Similarly, $k_{\text{-OCl,AA}}$ (0.047 $M^{-1}s^{-1}$) was obtained from the chlorine decrease in excess of AA at pH 10 (Table S3). At pH 10, the sum of chlorine and *N*-Cl-AA concentrations was constant during 60 min and equal to the initial chlorine concentration (Fig. S19). This suggests that *N*-Cl-AA is stable in presence of $^{-}$OCl, and therefore $k_{\text{-OCl},N\text{-Cl-AA}}$ is negligible. In addition, in contrast to *N*-Cl-BA, a self-decay of *N*-Cl-AA ($k_{N\text{-Cl-AA}}$) was not observed in the tested pH range 7–10 (Fig. S19). Lastly, $k_{\text{HOCl,AA}}$ and $k_{\text{HOCl},N\text{-Cl-AA}}$ were determined by simultaneously fitting to chlorine decrease and *N*-Cl-AA evolution at pH 7 by using $k_{\text{HOCl,AA}}$ and $k_{\text{HOCl},N\text{-Cl-AA}}$ as fitting parameters. As shown in Figure S20, the scenario analyses suggest optimal values of 0.008 $M^{-1}s^{-1}$ and 9 $M^{-1}s^{-1}$ for $k_{\text{HOCl,AA}}$ and $k_{\text{HOCl},N\text{-Cl-AA}}$, respectively. Applying the obtained rate constants (Table S2), the chlorine decrease

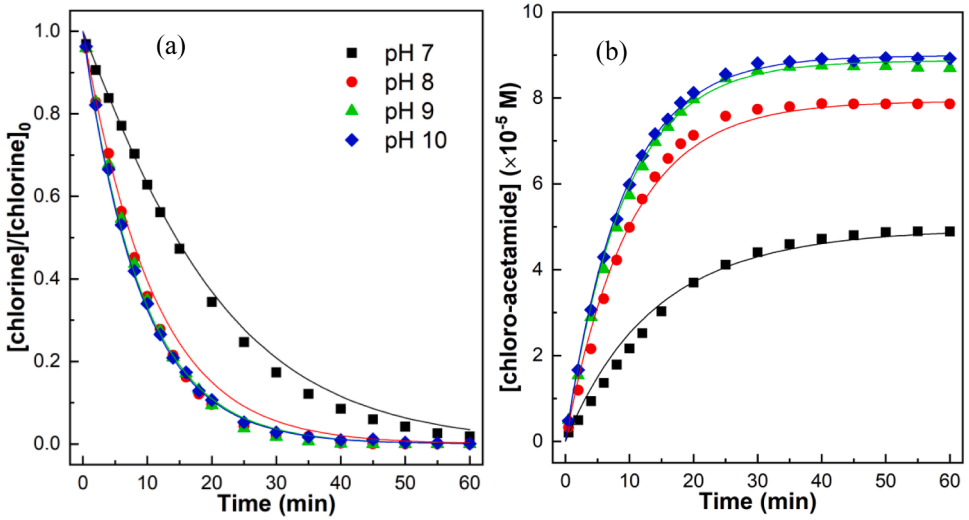

Fig. 4. Reaction of acetamide with chlorine at different pH values at 23 °C: Experimental data and modeling results. (a) Normalized chlorine residual concentration and (b) *N*-Cl-acetamide evolution. Lines represent model predictions (see text) and symbols are measured data. $[Chlorine]_0$ = 90 μM, $[acetamide]_0$ = 40 mM.

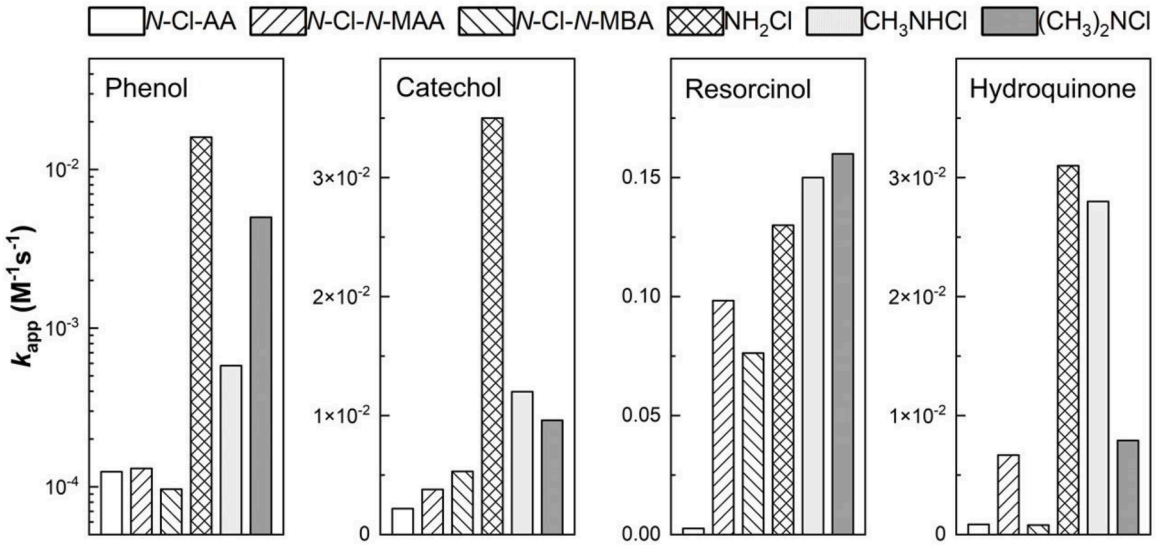

Fig. 5. Apparent second-order rate constants at pH 7 for reactions of different phenolic compounds (phenol, catechol, resorcinol, hydroquinone) with *N*-Cl-acetamide, *N*-Cl-*N*-methylacetamide, and *N*-Cl-*N*-methylbenzamide in comparison with chloramines (Heeb et al. 2017). Table S5 provides detailed experimental conditions and values for the second-order rate constants.

and *N*-Cl-AA evolution were well estimated for different pH values (Fig. 4).

3.5. Influence of bromide on the chlorination of amides

Under oxidative water treatment processes, bromide can play a critical role because bromide is converted to reactive bromine species (e.g., hypobromous acid/hypobromite, HOBr/$^{-}$OBr) which react fast with many inorganic and organic compounds (Heeb et al., 2014). HOBr reacts with amides with apparent second-order rate constants on the order of 1-3 $M^{-1}s^{-1}$ at pH 7.2-7.5 (Pattison and Davies, 2004). The influence of bromide on the chlorination of amides was assessed under typical water treatment conditions with 1 mg/L chlorine (as Cl_2) and varying bromide concentrations (10, 100, and 500 μg/L) by comparing the formation yield of chloramide and bromamide (Text S8). As shown in Table S5, when HOBr is in excess of amide, ~ 40% of amide was estimated to transform to bromamide other than chloramide in the presence of 10 μg/L bromide and > 87% of amide yielded bromamide with bromide concentration higher than 100 μg/L. The formation of chloramide becomes gradually more important for chlorine concentrations > 1 mg/L and dominant when the amide concentration is higher than the bromide concentration (Table S5). This suggests that the role of bromide has to be assessed during chlorination of amides for practical water treatment conditions.

3.6. Kinetics and mechanisms of the reactions of N-chloramides with phenolic compounds

N-Cl-AA, *N*-Cl-*N*-MAA, and *N*-Cl-*N*-MBA were selected to investigate the kinetics of their reactions with phenolic compounds (phenol, catechol, resorcinol, and hydroquinone) under pseudo-first-order conditions (Table S6). Apparent second-order rate constants at pH 7 for the reactions of phenols with *N*-chloramides range from 9.7×10^{-5} to 9.8×10^{-2} $M^{-1}s^{-1}$ which are 1-2 orders of magnitude lower than the reactions with chloramines (Heeb et al., 2017) (Fig. 5). Comparing among different phenols, the k_{app}-values for the reactions of *N*-chloramides with different phenols increase in the order of phenol < hydroquinone ≈ catechol < resorcinol which is the same for chloramines (Heeb et al., 2017). As expected, resorcinol has the highest reactivity with two hydroxyl groups in meta position and phenol has the lowest reactivity with only one hydroxyl group (Criquet et al., 2015; Heeb et al., 2017). Similar k_{app}-values were obtained for both phenol and catechol when reacting with the three tested *N*-chloramides. A lower k_{app}-value (30-38 fold) was observed for resorcinol when reacting with *N*-Cl-AA in comparison with *N*-Cl-*N*-MAA and *N*-Cl-*N*-MBA, and a higher k_{app}-value (8 fold) was observed for hydroquinone when reacting with *N*-Cl-*N*-MAA in comparison with *N*-Cl-AA and *N*-Cl-*N*-MBA (Table S6). These observed differences in the k_{app}-values warrant further investigations.

To obtain mechanistic information on the reactions between *N*-chloramides and phenolic compounds, transformation products from the reaction of *N*-Cl-AA with phenol, resorcinol, and hydroquinone were analyzed by HPLC-UV (Text S2 for analytical method). In the reaction of *N*-Cl-AA with phenol and resorcinol, ring-chlorinated products were detected which suggests an electrophilic aromatic substitution. From the reaction of phenol with *N*-Cl-AA, 4-chlorophenol, and 2-chlorophenol were gradually formed as major reaction products, followed by formation of 2,4-dichlorophenol and 2,6-dichlorophenol for longer reaction times (>10 h) (Figure S21). For the reaction of resorcinol with *N*-Cl-AA, 4-chlororesorcinol and 2-chlororesorcinol were detected with 4-chlororesorcinol as the predominant reaction intermediate. During chlorination of resorcinol, a ratio of 3:1 was observed for the formation rate of 4-chlororesorcinol relative to 2-chlororesorcinol (Heasley et al., 1989; Rebenne et al., 1996). Further reaction of chlorinated resorcinol with *N*-Cl-AA leads to the formation of 4,6-dichlororesorcinol and 2,4-dichlororesorcinol (Fig. S22). Overall, the detected chlorinated phenols and chlorinated resorcinols only account for the partial loss of phenol and resorcinol, for instance, when 40% (~16 μM) of phenol and resorcinol were abated, 2-8 μM chlorinated phenolic products were detected. Therefore, significant fractions of other transformation products, including ring cleavage products, must be formed, which were not identified in this study (Acero et al., 2005a; Arnold et al., 2008).

In the reaction of *N*-Cl-AA with hydroquinone, chlorinated hydroquinones were not detected. Instead, *p*-benzoquinone was detected as the only major reaction product which suggests an electron transfer reaction mechanism (Fig. S23). The reaction between *N*-Cl-AA and catechol was monitored spectrophotometrically and no obvious *o*-quinone peak was observed (λ_{max} at 390 nm, Criquet et al., (2015)) which is potentially due to relatively slow reaction between *N*-Cl-AA and catechol and the instability of *o*-quinone. Overall, similar to free chlorine and chloramines (Criquet et al., 2015; Heeb et al., 2017), phenol and resorcinol react with *N*-chloramides mainly via electrophilic aromatic substitution, and hydroquinone reacts mainly via electron

transfer.

Besides phenolic transformation products, the fate of the *N*-chloramides was also monitored in the reaction of *N*-Cl-*N*-MBA with phenols. *N*-Cl-*N*-MBA was chosen in this case because *N*-Cl-*N*-MBA and *N*-MBA can be monitored by HPLC-UV. *N*-Cl-*N*-MBA was observed to be fully transformed to *N*-MBA after reacting with different phenolic compounds with an excellent mass balance (Fig. S24, Scheme 1). Therefore, Cl-amides can serve as a temporary reservoir for active chlorine.

4. Conclusions

The kinetics and mechanisms of the chlorination of amides and the reactions of *N*-chloramides with phenolic compounds have been investigated. The main outcomes of this study are:

- Chlorination of amides is dominated by $^{-}$OCl via forming a hydrogen bond between amido hydrogen and the oxygen in $^{-}$OCl with species-specific second-order rate constants (k_{-OCl}) in the range of 7.3×10^{-3} – 2.3 $M^{-1}s^{-1}$. An electron-donating group at the amide-*N* and/or the *N*-carbonyl-*C* partially compensate the electron-withdrawing effect of the carbonyl group on the amide-*N* enhancing the strength of the *N*-*H* bond. This leads to a lower tendency to form a hydrogen bond with lower second-order rate constant for the reaction with $^{-}$OCl, e.g., $k_{-OCl,BA} > k_{-OCl,N\text{-}MBA} > k_{-OCl,N\text{-}PBA}$.
- Chlorination of both primary and secondary amides forms *N*-chloramides. *N*-Chlorinated primary amides undergo further chlorination, mainly by reacting with HOCl with higher second-order rate constants (~10 $M^{-1}s^{-1}$) than the first chlorination step. This is due to a weakening of the *N*-*H* bond and an enhanced reactivity with the electrophilic HOCl. In the presence of bromide, the formation of bromamides in addition of chloramides can be significant due to a higher reactivity of HOBr with amides.
- Activation energies for the chlorination of amides are in the range of 62–88 kJ/mol similar to the chlorination of *α,β*-unsaturated carbonyls. The chlorination of both compound classes is dominated by reaction with $^{-}$OCl. In contrast lower activation energies are obtained for moieties such as neutral amines, reduced sulfur and activated aromatic compounds, for which the reactions occur mainly with HOCl.
- *N*-Chloramides react with phenol and resorcinol via electrophilic aromatic substitution and with hydroquinone via electron transfer. The amides are recycled after reacting with phenols. Apparent second-order rate constant for the reactions of phenolic compounds with *N*-chloramides are in the order of 10^{-4}–0.1 $M^{-1}s^{-1}$, slightly lower than for chloramines (6×10^{-4} – 0.16 $M^{-1}s^{-1}$) and 3–5 orders of magnitude lower than for chlorine (18 - 4×10^{3} $M^{-1}s^{-1}$) (Criquet et al. 2015, Heeb et al. 2017).

Declaration of Competing Interest

The authors declare that they have no known competing financial interests or personal relationships that could have appeared to influence the work reported in this paper.

Data availability

Data will be made available on request.

Acknowledgments

We acknowledge funding from the Swiss Agency for Development and Cooperation (Project No. 7F-10345.03.01) for funding. We also thank Caroline Gachet-Acquillon for her valuable assistance in the laboratory and Florian Breider and Dominique Grandjean for the support with LC-MS analysis.

Supplementary materials

Supplementary material associated with this article can be found, in the online version, at doi:10.1016/j.watres.2023.120131.

References

Acero, J.L., Benitez, F.J., Real, F.J., Roldan, G., 2010. Kinetics of aqueous chlorination of some pharmaceuticals and their elimination from water matrices. Water Res. 44 (14), 4158–4170.
Acero, J.L., Benitez, F.J., Real, F.J., Roldan, G., Rodriguez, E., 2013. Chlorination and bromination kinetics of emerging contaminants in aqueous systems. Chem. Eng. J. 219, 43–50.
Acero, J.L., Piriou, P., von Gunten, U., 2005a. Kinetics and mechanisms of formation of bromophenols during drinking water chlorination: assessment of taste and odor development. Water Res. 39 (13), 2979–2993.
Acero, J.L., Rodriguez, E., Meriluoto, J., 2005b. Kinetics of reactions between chlorine and the cyanobacterial toxins microcystins. Water Res. 39 (8), 1628–1638.
Antelo, J.M., Arce, F., Parajó, M., Pousa, A.I., Pérez-moure, J.C., 1995. Chlorination of *N*-methylacetamide: a kinetic study. Int. J. Chem. Kinet. 27 (10), 1021–1031.
Arnold, W.A., Bolotin, J., von Gunten, U., Hofstetter, T.B., 2008. Evaluation of functional groups responsible for chloroform formation during water chlorination using compound specific isotope analysis. Environ. Sci. Technol. 42, 7778–7785.
Arrhenius, S., 1889. Über die Reaktionsgeschwindigkeit bei der Inversion von Rohrzucker durch Säuren [Reaction rate in inversion of cane sugar by acids]. Z. Phys. Chem. 4, 226–248.
Baird, R., Bridgewater, L., 2017. Standard Methods for the Examination of Water and Wastewater. American Public Health Association, Washington, D.C.
Barber, L.B., Leenheer, J.A., Noyes, T.I., Stiles, E.A., 2001. Nature and transformation of dissolved organic matter in treatment wetlands. Environ. Sci. Technol. 35, 4805–4816.
Berens, M.J., Capel, P.D., Arnold, W.A., 2021. Neonicotinoid insecticides in surface water, groundwater, and wastewater across land-use gradients and potential effects. Environ. Toxicol. Chem. 40 (4), 1017–1033.
Bexfield, L.M., Belitz, K., Lindsey, B.D., Toccalino, P.L., Nowell, L.H., 2021. Pesticides and pesticide degradates in groundwater used for public supply across the United States: Occurrence and human-health context. Environ. Sci. Technol. 55 (1), 362–372.
Corbett, J.F., 1972. Pseudo first-order kinetics. J. Chem. Educ. 49 (10), 663.
Criquet, J., Rodriguez, E.M., Allard, S., Wellauer, S., Salhi, E., Joll, C.A., von Gunten, U., 2015. Reaction of bromine and chlorine with phenolic compounds and natural organic matter extracts–Electrophilic aromatic substitution and oxidation. Water Res. 85, 476–486.
Deborde, M., von Gunten, U., 2008. Reactions of chlorine with inorganic and organic compounds during water treatment-kinetics and mechanisms: a critical review. Water Res. 42 (1-2), 13–51.
Ding, S., Chu, W., Krasner, S.W., Yu, Y., Fang, C., Xu, B., Gao, N., 2018. The stability of chlorinated, brominated, and iodinated haloacetamides in drinking water. Water Res. 142, 490–500.
Ferrer, I., Thurman, E.M., Barcelo, D., 2000. First LC-MS determination of cyanazine amide, cyanazine acid, and cyanazine in groundwater samples. Environ. Sci. Technol. 34, 714–718.
Ghose, A.K., Viswanadhan, V.N., Wendoloski, J.J., 1999. A knowledge-based approach in designing combinatorial or medicinal chemistry libraries for drug discovery. 1. A qualitative and quantitative characterization of known drug databases. J. Comb. Chem. 1, 55–68.
Hardy, F.E., Robson, P., 1967. The formation and hydrolysis of substituted *N*-chloro-*N*-methylbenzamides in aqueous alkali. J. Chem. Soc. B 1151–1154.
Hargreaves, A.E., 2003. Chemical formulation: An Overview of Surfactant Based Chemical Preparations Used in Everyday Life. Royal Society of Chemistry.
Harrison, R.M., Perry, R., Wellings, R.A., 1976. Chemical kinetics of chlorination of some polynuclear aromatic hydrocarbons under conditions of water treatment processes. Environ. Sci. Technol. 10 (12), 1156–1160.
Heasley, V.L., Burns, M.D., Kemalyan, N.A., Mckee, T.C., Schroeter, H., Teegarden, B.R., Whitney, S.E., Wershaw, R.L., 1989. Aqueous chlorination of resorcinol. Environ. Toxicol. Chem. 8 (12), 1159–1163.
Heeb, M.B., Criquet, J., Zimmermann-Steffens, S.G., von Gunten, U., 2014. Oxidative treatment of bromide-containing waters: Formation of bromine and its reactions with inorganic and organic compounds - A critical review. Water Res. 48, 15–42.
Heeb, M.B., Kristiana, I., Trogolo, D., Arey, J.S., von Gunten, U., 2017. Formation and reactivity of inorganic and organic chloramines and bromamines during oxidative water treatment. Water Res. 110, 91–101.
Hu, C.Y., Cheng, M., Lin, Y.L., 2015. Chlorination of bensulfuron-methyl: kinetics, reaction factors and disinfection by-product formation. J. Taiwan Inst. Chem. Eng. 53, 46–51.
Hu, C.Y., Lin, Y.L., Li, A.P., Xu, B., 2018. Degradation kinetics and disinfection by-product formation of chlorimuron-ethyl during aqueous chlorination. Sep. Purif. Technol. 204, 49–55.
Hu, C.Y., Zhang, J.C., Lin, Y.L., Ren, S.C., Zhu, Y.Y., Xiong, C., Wang, Q.B., 2021. Degradation kinetics of prometryn and formation of disinfection by-products during chlorination. Chemosphere 276, 130089.
Johnson, M., Melbourne, P., 1996. Photolytic spectroscopic quantification of residual chlorine in potable waters. Analyst 121, 1075–1078.

Kolpin, D.W., Thurman, E.M., Goolsby, D.A., 1996. Occurrence of selected pesticides and their metabolites in near-surface aquifers of the midwestern United States. Environ. Sci. Technol. 30, 335–340.
Lee, G.F., Morris, J.C., 1962. Kinetics of chlorination of phenol-chlorophenolic tastes and odors. Int. J. Air Wat. Poll. 6, 419–431.
Leenheer, J.A., Croue, J.P., 2003. Characterizing aquatic dissolved organic matter. Environ. Sci. Technol. 1, 18A–26A.
Li, J., Jiang, J., Manasfi, T., von Gunten, U., 2020. Chlorination and bromination of olefins: Kinetic and mechanistic aspects. Water Res. 187, 116424.
Logan, S.R., 1982. The origin and status of the Arrhenius equation. J. Chem. Educ. 59 (4), 279–281.
Marron, E.L., Van Buren, J., Cuthbertson, A.A., Darby, E., von Gunten, U., Sedlak, D.L., 2021. Reactions of α,β-unsaturated carbonyls with free chlorine, free bromine, and combined chlorine. Environ. Sci. Technol. 55 (5), 3305–3312.
Mauger, R.P., Soper, F.G., 1946. Acid catalysis in the formation of chloroamides from hypochlorous acid. N-chlorination by hypochlorite ions and by acyl hypochlorites. J. Chem. Soc. 71–75.
Morris, J.C., 1966. The acid ionization constant of HOCl from 5 to 35°. J. Phys. Chem. 70, 3798–3805.
Morris, J.C., 1967. Kinetics of Reactions Between Aqueous Chlorine and Nitrogen Compounds. Wiley, New York.
Morris, J.C., 1978. The Chemistry of Aqueous Chlorine in Relation to Water Chlorination. Ann Arbor Science Publishers, Michigan.
Muellner, M.G., Wagner, E.D., Mccalla, K., Richardson, S.D., Woo, Y.-T., Plewa, M.J., 2007. Haloacetonitriles vs. regulated haloacetic acids: are nitrogen-containing DBPs more toxic? Environ. Sci. Technol. 41, 645–651.
Pattison, D.I., Davies, M.J., 2004. Kinetic analysis of the reactions of hypobromous acid with protein components: implications for cellular damage and use of 3-bromotyrosine as a marker of oxidative stress. Biochemistry 43, 4799–4809.
Pico, Y., Blasco, C., Font, G., 2004. Environmental and food applications of LC-tandem mass spectrometry in pesticide-residue analysis: an overview. Mass Spectrom. Rev. 23 (1), 45–85.
Plewa, M.J., Muellner, M.G., Richardson, S.D., Fasano, F., Buettner, K.M., Woo, Y.T., Mckague, B., Wagner, E.D., 2008. Occurrence, synthesis, and mammalian cell cytotoxicity and genotoxicity of haloacetamides: an emerging class of nitrogenous drinking water disinfection byproducts. Environ. Sci. Technol. 42, 955–961.
Prutz, W.A., 1999. Consecutive halogen transfer between various functional groups induced by reaction of hypohalous acids: NADH oxidation by halogenated amide groups. Arch. Biochem. Biophys. 371, 107–114.
Rebenne, L.M., Gonzalez, A.C., Olson, T.M., 1996. Aqueous chlorination kinetics and mechanism of substituted dihydroxybenzenes. Environ. Sci. Technol. 30, 2235–2242.
Rodriguez, E., Sordo, A., Metcalf, J.S., Acero, J.L., 2007. Kinetics of the oxidation of cylindrospermopsin and anatoxin-a with chlorine, monochloramine and permanganate. Water Res. 41 (9), 2048–2056.
Sivey, J.D., Mccullough, C.E., Roberts, A.L., 2010. Chlorine monoxide (Cl_2O) and molecular chlorine (Cl_2) as active chlorinating agents in reaction of dimethenamid with aqueous free chlorine. Environ. Sci. Technol. 44, 3357–3362.
Snider, E.H., Alley, F.C., 1979. Kinetics of the chlorination of biphenyl under conditions of waste treatment processes. Environ. Sci. Technol. 13 (10), 1244–1248.
Stalter, D., O'Malley, E., von Gunten, U., Escher, B.I., 2016. Fingerprinting the reactive toxicity pathways of 50 drinking water disinfection by-products. Water Res. 91, 19–30.
Thomm, E.W.C.W., Wayman, M., 1969. N-chlorination of secondary amides II. Effects of substituents on rates of N-chlorination. Can. J. Chem. 47, 3289–3297.
Urano, K., Wada, H., Takemasa, T., 1983. Empirical rate equation for trihalomethane formation with chlorination of humic substances in water. Water Res. 17 (12), 1797–1802.
Wang, T.X., Kelley, M.D., Cooper, J.N., Beckwith, R.C., Margerum, D.W., 1994. Equilibrium, kinetic, and UV-spectral characteristics of aqueous bromine chloride, bromine, and chlorine species. Inorg. Chem. 33, 5872–5878.
Xu, B., Gao, N.Y., Cheng, H., Hu, C.Y., Xia, S.J., Sun, X.F., Wang, X., Yang, S., 2009. Ametryn degradation by aqueous chlorine: kinetics and reaction influences. J. Hazard. Mater. 169 (1-3), 586–592.
Yu, Y., Reckhow, D.A., 2017. Formation and occurrence of N-chloro-2,2-dichloroacetamide, a previously overlooked nitrogenous disinfection byproduct in chlorinated drinking waters. Environ. Sci. Technol. 51 (3), 1488–1497.
Zhang, Q., Pehkonen, S.O., 1999. Oxidation of diazinon by aqueous chlorine: Kinetics, mechanisms, and product studies. J. Agric. Food Chem. 47, 1760–1766.